THE JOURNAL OF PHYSICAL CHEMISTRY A

Subscriber access provided by UNIV OF NOTTINGHAM

A: Spectroscopy, Molecular Structure, and Quantum Chemistry

# Möbius and Hückel Cyclacenes with Dewar and Ladenburg Defects

Magnus W.D. Hanson-Heine, and Jonathan Darrell Hirst

*J. Phys. Chem. A*, **Just Accepted Manuscript** • DOI: 10.1021/acs.jpca.0c04137 • Publication Date (Web): 14 Jun 2020

# Möbius and Hückel Cyclacenes with Dewar and Ladenburg Defects

**Magnus W. D. Hanson-Heine* and Jonathan D. Hirst**

*School of Chemistry, University of Nottingham, University Park, Nottingham NG7 2RD.*

**magnus.hansonheine@nottingham.ac.uk*

**Abstract:** Cyclacene nanobelts have not been synthesized in over 60 years and remain one of the last unsynthesized building blocks of carbon nanotubes. Recent work has predicted that Hückel-cyclacenes containing Dewar benzenoid ring isomers are the most stable isomeric forms for several of the smaller sizes of cyclacene belt. Here we give a more complete picture of the isomers that are possible within these nanobelt systems by simulating embedded Ladenburg (prismane) benzenoid rings in Hückel-[n]cyclacenes (*n* = 5-14), and embedded Dewar benzenoid rings in twisted Möbius-[n]cyclacenes (*n* = 9-14). The Möbius-[9]cyclacene isomer containing one Dewar benzenoid defect, and the Hückel-[5]cyclacene isomer containing two maximally spaced Ladenburg benzenoid defects, are found to be more stable than their conventional Kekulé benzenoid ring counterparts. The isomers that contain Dewar and Ladenburg benzenoid rings have larger electronic singlet-triplet energy gaps and lower polyradical character when compared with the conventional isomers.

**TOC Graphic:**

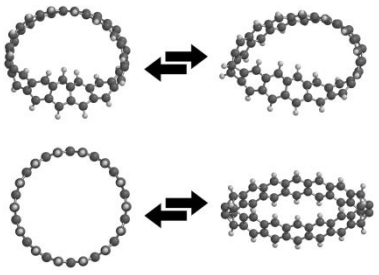

## Introduction

Hückel-cyclacenes were first reported in the literature by Heilbronner in 1954.[1-2] They can be considered as being either an arenoid belt made up of fused benzene rings or two fused trans-polyene ribbons,[3] where the odd numbers of fused rings show a lower relative stability.[4] Cyclacenes are the last minimal building block of carbon nanotubes to remain unsynthesized. Itami and co-workers managed to synthesize a related chiral carbon nanobelt in 2017,[5] but attempts at making cyclacenes have remained unsuccessful to date.[6-10] The synthetic challenges may arise from the high ring strain in the smaller cyclacenes or have their origins in the predicted low energy triplet electronic states and significant polyradical character in the ground states of the larger belt sizes.[11-13] A more complete understanding of cyclacene behaviour could, therefore, aid in the understanding of carbon nanotubes[14-16] and may help to guide future synthetic strategies.

In 1964 Heilbronner also proposed that organic polyene ribbons could accommodate a twist (or knot) in their structure to become a Möbius band with one edge topologically.[17] Since then various organic and inorganic Möbius belt shaped molecules have been synthesized.[18-21] Möbius rings and nanobelts are predicted to have a range of interesting electronic properties. Hückel rules for aromaticity are no longer predicted to be valid for Möbius polyene belts,[18] and Möbius-[n]cyclacenes have been characterized as having an anti-aromatic polyene rim for all ring sizes. This stands in contrast to the unknotted Hückel-[n]cyclacenes, which have upper and lower aromatic polyene ribbons for the belts comprising an odd number of benzenoid rings and anti-aromatic polyene ribbons for belts with an even number.[22] Möbius-[n]cyclacenes have torus screw rotation symmetry in addition to $C_2$ symmetry.[23] The π-electrons of the Möbius-[n]cyclacenes are relatively localized in the twisted region of the ring, with molecular dynamics calculations of Möbius-[11]cyclacene indicating that the Möbius twist travels around the belt at room temperature with a period on the order of several picoseconds, causing a temperature dependent spin current associated with the magnetic moment of the twist.[24] Despite having consistently antiaromatic polyene ribbons, the first hyperpolarizabilities of the Möbius-[n]cyclacenes ($n$ = 13-18) oscillate in a zigzag pattern for belts made up of even or odd number of benzenoid rings.[25] Möbius-[8]cyclacene has also been predicted to facilitate spiral charge transfer when used as a conjugated bridge in a donor-π-

conjugated bridge-acceptor framework.[26-27] Analysis of the frontier molecular orbitals in the *n* = 13-18 systems suggests that the lowest electronic excited states involve electron transfer from the twisted areas of these belts to the un-twisted areas when the belts are made up of an even number of benzenoid rings, but that the reverse is true for belts made up of an odd number of benzenoid rings.[25] As with the Hückel-[n]cyclacenes, single reference Kohn-Sham density functional theory (DFT) calculations have found electronic ground states with triplet multiplicity for various Möbius-[n]cyclacenes.[28-29] However, studies using thermally-assisted-occupation density functional theory (TAO-DFT) have shown this is likely an artefact arising from the neglect of static correlation, and have predicted singlet ground states for Möbius-[n]cyclacenes where *n* = 8-100.[29]

Isolated benzene rings can undergo interconversion into a range of ring isomers in addition to the stable aromatic structure proposed by Kekulé.[30-33] These structures include bicyclo[2.2.0]-hexa-2,5-diene and tetracyclo[2.2.0.$0^{2,6}$.$0^{3,5}$]hexane, otherwise known as Dewar benzene and Ladenburg benzene (or prismane), shown in Figure 1. Hanson-Heine et al. recently found evidence that isomers containing a small number of Dewar benzenoid rings are more stable than the conventional structures that contain only contain Kekulé benzenoid rings when considering several of the smaller Hückel-cyclacene belt sizes.[34] These Dewar benzenoid ring containing isomers are predicted to have less polyradical character and higher singlet-triplet stabilities than the conventional cyclacene isomers, and therefore represent potentially stable synthetic targets.

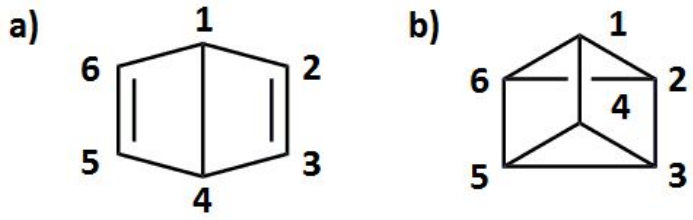


Figure 1. Chemical structures of a) Dewar benzene and b) Ladenburg benzene (prismane).

Möbius and Dewar benzenoid ring rearrangements are chemically interesting aspects of cyclacene behaviour in their own right and form part of a more complete understanding of cyclacene chemistry. This study, therefore, aims to examine the properties that are introduced when these rearrangements are coincident, and

produce Dewar benzenoid ring containing Möbius-[n]cyclacenes. Furthermore, as cyclacene benzenoid rings share some of the isomerizations available to molecular benzene, we also test whether the introduction of Ladenburg defects produces a similar set of effects to the Dewar defects when introduced into Hückel-[n]cyclacene systems.

## Methods

Density functional theory calculations were performed using a developmental version of the Q-Chem 5 software.[35] Optimized geometries were calculated for isomers of the Möbius-[n]cyclacenes (*n* = 9-14) containing both one Dewar benzenoid ring and purely Kekulé benzenoid rings, and for the Hückel-[n]cyclacenes (*n* = 5-14) containing one or two Ladenburg benzenoid rings, using unrestricted DFT with the B3LYP exchange-correlation functional and the 6-31G(d) basis set.[36-37] Minima were confirmed through the absence of imaginary harmonic frequencies. The symmetry of the initial wave function was broken by adding 10% of the lowest unoccupied molecular orbital (LUMO) to the highest occupied molecular orbital (HOMO). Hückel- and Möbius-[n]cyclacenes have significant static electron correlation. Therefore, TAO-DFT[38] was used to characterize the properties at these optimized geometries. TAO-DFT is designed to deal with strong static correlation effects and has a similar accuracy to *ab initio* multi-reference methods when calculating zigzag graphene nanoribbons,[39] polyacenes,[40] the Kekulé benzenoid ring and Dewar benzenoid ring containing isomers of Hückel-[n]cyclacenes,[34, 41] and the conventional Möbius-[n]cyclacenes.[29] TAO-DFT can also accurately capture multireference character in molecular vibrational frequencies.[42] Studies have indicated that the orbital occupation numbers from TAO-DFT are qualitatively similar to the natural orbital occupation numbers in high-level multi-reference methods, and can, thus, be used to assess polyradical character.[38-39, 43-44] Relative energies and orbitals were calculated at the optimized geometries using TAO-DFT with the PBE exchange-correlation functional at a fictitious temperature of $\theta = 7\times10^{-3}$ $E_h$ in combination with the local density approximation fictitious temperature-dependent energy functional developed by Chai,[38] and the 6-311+G(2df,2p) basis set.[38, 40] The PBE functional can overestimate electron delocalization, with possible effects on the singlet-triplet

relative stabilities of certain systems. However, TAO-PBE has previously been found to be accurate for calculations of polyacenes, Dewar benzenoid ring containing Hückel-cyclacenes, and both the Hückel and Möbius isomers of conventional cyclacenes. Vertical singlet-triplet state energy gaps were calculated from the differences between the self-consistent field energies of the lowest singlet and lowest triplet electronic states.

## Results and Discussion

### Isomer Stabilities

The relative stabilities of the Hückel-[n]cyclacene isomers that also contain Ladenburg benzenoid rings have been assessed using energy calculations performed on the isomers with one and two Ladenburg benzenoid rings, as depicted for Hückel-[14]-cyclacene in Figure 2. The different positions that two Ladenburg benzenoid rings can occupy relative to each other in a cyclacene will lead to structures with different energies. Following the observations made for the Dewar benzenoid ring containing cyclacene isomers, these calculations have been performed with the two Ladenburg benzenoid rings located on opposite sides of the molecule.[34] These energies, shown in Table 1, have been compared against with the equivalent structures for the isomers containing Dewar benzenoid rings, and the isomers with only Kekulé benzenoid rings that have previously been reported in the literature. The Hückel-[5]cyclacene isomer with two Ladenburg benzenoid rings is more stable than the purely Kekulé benzenoid ring isomer, and the previously identified isomers containing two Dewar benzenoid rings remain the lowest energy isomers for the $n$ = 5-7 belt sizes, with the isomers containing with two Ladenburg benzenoid rings being ca. 16, 28, and 39 kcal mol$^{-1}$ higher in energy, respectively.

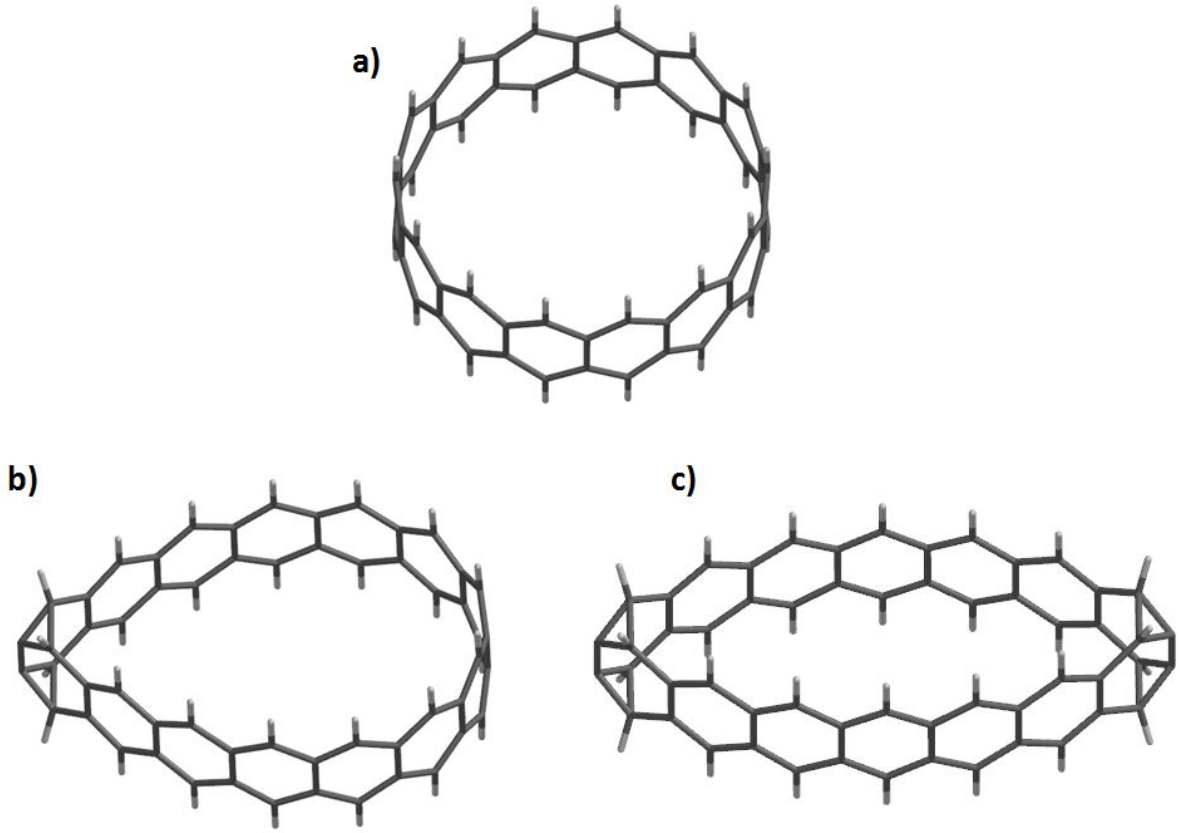


Figure 2. Optimized geometries of the 14-cyclacene isomers studied containing a) only Kekulé benzenoids, b) one Ladenburg benzenoid, and c) two Ladenburg benzenoids.

Table 1. Relative energies in kcal mol$^{-1}$ for the Hückel-[n]cyclacene isomers containing different numbers of Kekulé benzenoid (KB), Ladenburg benzenoid (LB) and Dewar benzenoid (DB) structures given in parentheses.

| *n* | LB(1) | LB(2) | DB(1)[a] | DB(2)[a] | KB only [a] |
|---|---|---|---|---|---|
| 5 | 54.5 | 16.4 | 26.7 | 0.0 | 45.0 |
| 6 | 46.3 | 27.8 | 17.6 | 0.0 | 14.2 |
| 7 | 37.8 | 39.1 | 10.9 | 0.0 | 11.4 |
| 8 | 51.3 | 58.4 | 21.1 | 16.9 | 0.0 |
| 9 | 40.2 | 59.7 | 11.8 | 13.6 | 0.0 |
| 10 | 57.7 | 76.8 | 27.4 | 34.5 | 0.0 |
| 11 | 50.9 | 79.1 | 20.1 | 33.4 | 0.0 |
| 12 | 60.9 | 90.9 | 28.9 | 46.4 | 0.0 |
| 13 | 60.3 | 96.7 | 28.6 | 50.2 | 0.0 |
| 14 | 61.5 | 102.5 | 31.2 | 55.5 | 0.0 |

[a]data taken from ref.[34]

Due to the inherently higher energies and the additional structural complexity introduced by the knot in Möbius systems, Ladenburg defects have not been considered for with Möbius-[n]cyclacenes, and we have instead chosen to focus on

isomers containing the less angular Dewar benzenoid defects. Energy calculations have been performed on the Möbius-[n]cyclacene isomers with up to one Dewar benzenoid ring, due to ring strain considerations. Preliminary geometry optimizations found that the ring twist consistently migrated until reaching the Dewar benzenoid ring structure, giving the relative positions shown for Möbius-[14]cyclacene in Figure 3. Cartesian coordinates and absolute energies for the optimized geometries of all isomers considered in this work are provided in the Supporting Information. The relative energies for these isomers, shown in Table 2, indicate that the Möbius-[9]cyclacene containing a Dewar benzenoid ring is more stable than the equivalent purely Kekulé isomer, and that the purely Kekulé isomer of Möbius-[10]cyclacene is only ca. 1.6 kcal $mol^{-1}$ more stable than its Dewar benzenoid ring counterpart. Furthermore, the relative energies of the Möbius-[n]cyclacenes that contain Dewar benzenoid rings are consistently 10 kcal $mol^{-1}$ lower than the relative energies of the Hückel-[n]cyclacenes with Dewar benzenoid rings, when each are considered relative to their equivalent size of Kekulé-only isomer for the Hückel and Möbius systems, respectively. This suggests that the Dewar benzenoid rings act to reduce the strain introduced by the Möbius twist in partial compensation for the increased strain when forming the Dewar benzenoid ring structure. However, the Möbius-[n]cyclacenes still have energies > 87 kcal $mol^{-1}$ above the equivalent Hückel-[n]cyclacenes for all of the systems studied.

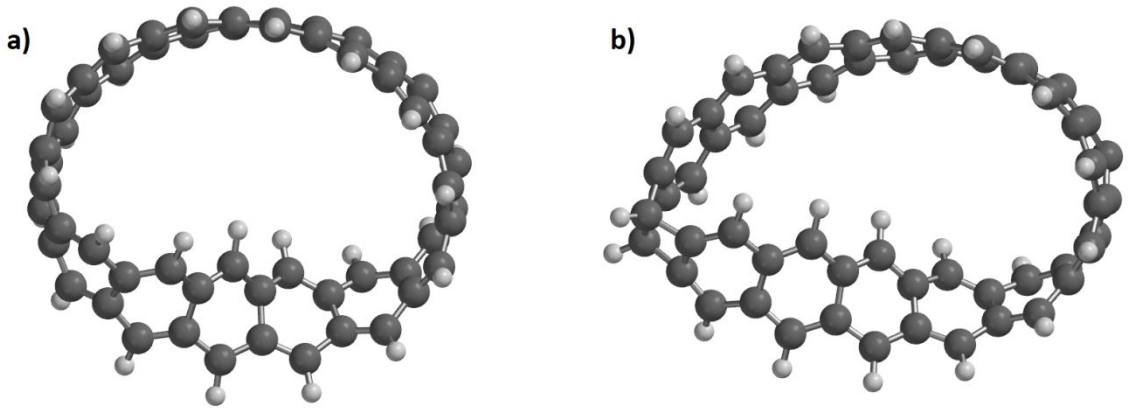


Figure 3. Optimized geometries of the Möbius-[14]cyclacene isomers studied containing a) Kekulé benzenoid rings only and b) a single Dewar benzenoid ring.

Table 2. Relative energies in kcal mol$^{-1}$ for the Hückel-[n]cyclacene and Möbius-[n]cyclacene isomers with a Dewar benzenoid ring, relative to their Kekulé-only counterparts.

| *n* | Möbius-[n]cyclacene | Hückel-[n]cyclacene[a] |
|---|---|---|
| 9 | -1.6 | 11.8 |
| 10 | 1.6 | 27.4 |
| 11 | 4.9 | 20.1 |
| 12 | 10.1 | 28.9 |
| 13 | 11.9 | 28.6 |
| 14 | 16.3 | 31.2 |

[a]data taken from ref.[34]

## Singlet-Triplet Energy Gaps

Table 3. Singlet-Triplet vertical transition energies in eV for the Hückel-[n]cyclacene isomers containing different numbers of Kekulé benzenoid rings (KB), Ladenburg benzenoid (LB), and Dewar benzenoid (DB) structures given in parentheses.

| *n* | LB(1) | LB(2) | DB(1)[a] | DB(2)[a] | KB only[a] |
|---|---|---|---|---|---|
| 5 | 0.59 | 1.85 | 0.53 | 1.94 | 0.28 |
| 6 | 0.86 | 2.09 | 0.65 | 1.70 | 0.39 |
| 7 | 0.82 | 1.97 | 0.56 | 1.64 | 0.22 |
| 8 | 0.58 | 1.96 | 0.40 | 1.26 | 0.45 |
| 9 | 0.48 | 1.66 | 0.32 | 1.11 | 0.08 |
| 10 | 0.33 | 1.50 | 0.26 | 0.87 | 0.36 |
| 11 | 0.28 | 1.18 | 0.20 | 0.70 | 0.07 |
| 12 | 0.23 | 0.99 | 0.19 | 0.55 | 0.25 |
| 13 | 0.20 | 0.77 | 0.16 | 0.43 | 0.09 |
| 14 | 0.18 | 0.61 | 0.16 | 0.34 | 0.15 |

[a]data taken from ref.[34]

The Hückel-[n]cyclacene isomers containing Ladenburg benzenoid rings are predicted to have singlet electronic ground states with the singlet-triplet energy gaps shown in Table 3. The singlet-triplet energy gaps for the ground state configurations of the purely Kekulé Hückel-[n]cyclacenes oscillate due to the even belt sizes having more stable ground state configurations relative to the odd belt sizes. On the other hand, the isomers with one Ladenburg benzenoid ring do not show an oscillating pattern. These isomers have energy gaps that become comparable to the conventional even numbered Hückel-cyclacenes for the [8]cyclacene and upward. The isomers with two Ladenburg benzenoid rings have significantly larger singlet-triplet gaps than the isomers discussed so far, starting +1.57 eV above the purely

Kekulé isomer for [5]cyclacene, and following a nearly monotonically decreasing trend as the belt size increases.

Möbius-[n]cyclacenes with Dewar benzenoid rings are also predicted to have singlet electronic ground states and consistently larger singlet-triplet energy gaps when Dewar defects are introduced, ranging from +0.1 to +0.6 eV, shown in Table 4. The alternating excitation energies predicted for the Kekulé isomers with even and odd numbers of benzenoid rings for the Möbius-[11]cyclacene and larger belt sizes are in line with the frontier orbital analysis of Gao et al.[25] This discussion will therefore focus on the orbitals of the newly identified isomers shown in Figure 4. The excitation energies for the Möbius isomers with Dewar defects follows a similar alternating pattern, with a larger magnitude than for the purely Kekulé isomers of Möbius-[11]cyclacene and larger. This stands in contrast to the untwisted Hückel isomers, which do not show an oscillating excitation energy pattern in the isomers that contain Dewar structures. The smaller nanobelts have excitation energies that fall outside of this trend for $n$ = 11 and larger belts, which is attributed to an energetic reordering between the HOMO and the LUMO of the Dewar benzenoid ring containing isomers of the even numbered Möbius-[10]cyclacene and Möbius-[12]cyclacene belts. The Möbius-[9]cyclacene belt containing a Dewar benzenoid ring has a different HOMO to the orbitals seen for the larger belts with an odd number of benzenoid rings, and this is attributed to the increased ring strain at the smaller belt sizes. The lowest singlet to triplet energy gaps of greater than ca. 1.6 eV that are seen for the Hückel-[n]cyclacene isomers with two Dewar benzenoid rings where the belt size $n$ = 5-7, and for the isomers containing two Ladenburg benzenoid rings where $n$ = 5-9, suggest that the ground states of these Dewar and Ladenburg benzenoid ring species may be isolable under normal laboratory conditions. However, in the Ladenburg benzenoid ring case, the high relative energies for those isomers are likely to hinder their formation and isolation under ambient conditions.

Table 4. Singlet-Triplet vertical transition energies in eV for Möbius-[n]cyclacene isomers with and without a Dewar benzenoid (DB) defect.

| *n* | Möbius-[n]cyclacene (without DB) | Möbius-[n]cyclacene (with DB) |
|---|---|---|
| 9 | 0.15 | 0.17 |
| 10 | 0.17 | 0.23 |
| 11 | 0.16 | 0.22 |
| 12 | 0.14 | 0.16 |
| 13 | 0.13 | 0.19 |
| 14 | 0.12 | 0.13 |

## Radical Character

Conventional Hückel-[n]cyclacenes are known multireference systems that are predicted to possess a significant amount of polyradical character that anti-correlates strongly with their singlet-triplet energy gaps.[13] A high degree of polyradical character has also been predicted for the Möbius-[n]cyclacenes.[29] Multireference systems with strong static correlation have more orbitals with fractional occupation numbers, and radical character can therefore be estimated using the symmetrized von Neumann entropy (see equation 1), which has been used to calculate an approximate polyradical character of both Möbius and Hückel cyclacene isomers through the formula[20, 27, 29, 31]

$$S_{vN} = -\frac{1}{2}\sum_{i=1}^{\infty}\left[f_i \ln(f_i) + (1 - f_i)\ln(1 - f_i)\right], \qquad \mathbf{1}$$

where $f_i$ are the fractional occupation numbers.

The symmetrized von Neumann entropy is shown in Table 5 for the Hückel isomers and in Table 6 for the Möbius isomers. The purely Kekulé Hückel-cyclacenes have oscillating symmetrized von Neumann entropies in line with previous calculations, showing that belts with odd *n* have a greater degree of radical character than the even *n* belts when *n* is relatively small.[41] The symmetrized von Neumann entropies of the Hückel isomers with a single Ladenburg benzenoid ring do not oscillate and begin to follow a nearly linear trend with increasing size from the [8]cyclacene isomer

onwards, after an initial decrease in the symmetrized von Neumann entropy between the [5]cyclacene and [6]cyclacene isomers. These single Ladenburg benzenoid ring isomers give symmetrized von Neumann entropies that are close to the purely Kekulé cyclacenes for even *n* values once *n* is 8 or larger, and the symmetrized von Neumann entropy also appears to be anti-correlated to the singlet-triplet gaps, again suggesting a close relationship between the transition energy and the radical character. The overall trend is similar to that of the Hückel-[n]cyclacenes containing single Dewar benzenoid rings, although the value is consistently lower for the Ladenburg benzenoid ring containing isomers. The isomers containing two Ladenburg benzenoid rings also have relatively low symmetrized von Neumann entropies and are therefore likely to possess only a very limited radical character and static correlation. These isomers again follow a similar trend to their equivalent Dewar benzenoid ring containing isomers. However, the symmetrized von Neumann entropies increase more slowly for the larger Ladenburg benzenoid ring isomers, suggesting that the Ladenburg benzenoid ring isomers are likely to be well behaved when using single reference *ab initio* methods for larger sizes of nanobelt. The symmetrized von Neumann entropies for the isomers containing either two Ladenburg benzenoid rings or two Dewar benzenoid rings, both show a different trend to the singlet-triplet gaps, indicating that the relative stability of their singlet ground states are not significantly determined by the presence of radical character.

The symmetrized von Neumann entropies for the Möbius-[n]cyclacene isomers show an oscillating pattern that increases as a function of belt size from Möbius-[11]cyclacene onwards. The Dewar benzenoid ring containing isomers in this case show a similar trend, starting at a lower value that can be attributed to loss of aromaticity from the additional Kekulé benzenoid ring. The lower degree of correlation between the symmetrized von Neumann entropies and the singlet-triplet gaps seen for the Möbius-[n]cyclacenes compared to their Hückel-[n]cyclacene counterparts for *n* = 9-11, indicates that polyradical character is also a less important factor in determining the singlet-triplet energy gap for the smaller Möbius belt sizes.

To further examine the trends seen in the symmetrized von Neumann entropies, several sets of active orbital occupation numbers from the ground state TAO-DFT calculations are also shown in Table 7 and Table 8, where the $(N/2)^{th}$ orbital and the $(N/2+1)^{th}$ orbital are referred to as the HOMO and LUMO. Occupation numbers are

shown for the HOMO-2 to LUMO+2 as the occupation numbers of lower and higher energy orbitals, respectively, showed little change. The occupation numbers suggest that the radical character seen for the Hückel-[n]cyclacene isomers with only Kekulé benzenoid rings comes from oscillating occupancy swapping between the HOMO and HOMO-1 and the LUMO and LUMO+1, reaching a maximum of approximately 50 % occupancy in all four orbitals for the [11]cyclacene. The continued increase for the larger belt sizes then come from occupancy between the HOMO-2 and LUMO+2. The Kekulé-only Möbius-[n]cyclacenes show a more complex pattern over this range of belt sizes, but are known to show similar oscillating “wave-packet” behaviour for the larger sizes of nanobelt.[29]

By contrast, the symmetrized von Neumann entropies seen for the Hückel-[n]cyclacene with single Ladenburg benzenoid rings, are almost entirely due to orbital occupancy differences between the HOMO and LUMO. The HOMO occupancy only increases at the [14]cyclacene belt size, accompanied by a drop in the HOMO-1 occupation. The orbital occupations for the Hückel isomers with two Ladenburg isomers have not been tabulated due to having only small differences between the individual orbital occupations, with the [14]cyclacene HOMO orbital occupation remaining at 1.91. The Möbius-[n]cyclacenes with Dewar benzenoid rings, again follow a more complex pattern of occupations, with the drop in the symmetrized von Neumann entropy seen for the Möbius-[11]cyclacene coming primarily from a reduction in occupation numbers for the HOMO-1, HOMO, and LUMO.

Table 5. Symmetrized von Neumann entropy for the Hückel-[n]cyclacene isomers containing different numbers of Kekulé benzenoid (KB), Ladenburg benzenoid (LB), and Dewar benzenoid (DB) structures given in parentheses.

| *n* | LB(1) | LB(2) | DB(1)[a] | DB(2)[a] | KB only[a] |
|---|---|---|---|---|---|
| 5 | 0.641 | 0.047 | 0.751 | 0.032 | 1.356 |
| 6 | 0.360 | 0.031 | 0.595 | 0.063 | 0.968 |
| 7 | 0.414 | 0.033 | 0.733 | 0.066 | 1.589 |
| 8 | 0.711 | 0.036 | 1.067 | 0.185 | 0.939 |
| 9 | 0.926 | 0.064 | 1.271 | 0.221 | 2.571 |
| 10 | 1.251 | 0.094 | 1.474 | 0.411 | 1.204 |
| 11 | 1.423 | 0.193 | 1.708 | 0.553 | 2.804 |
| 12 | 1.624 | 0.297 | 1.793 | 0.809 | 1.737 |
| 13 | 1.806 | 0.491 | 2.007 | 1.057 | 2.812 |
| 14 | 1.941 | 0.704 | 2.128 | 1.344 | 2.474 |

[a]data taken from ref.[34] and doubled to account for both spin manifolds.

Table 6. Symmetrized von Neumann entropies for the Möbius-[n]cyclacene isomers with and without a Dewar benzenoid (DB) defect.

| *n* | Möbius-[n]cyclacene (without DB) | Möbius-[n]cyclacene (with DB) |
|---|---|---|
| 9 | 1.685 | 1.502 |
| 10 | 1.798 | 1.578 |
| 11 | 1.967 | 1.254 |
| 12 | 2.304 | 1.986 |
| 13 | 2.403 | 1.910 |
| 14 | 2.754 | 2.327 |

Table 7. Frontier active orbital occupation numbers for the TAO-DFT electronic structures of the Hückel-[n]cyclacene isomers with only Kekulé benzenoid rings (KB) and one Ladenburg benzenoid ring (LB). The occupations have been doubled in order to account for both spin densities.

| | Hückel KB | | | | | | Hückel LB | | | | | |
|---|---|---|---|---|---|---|---|---|---|---|---|---|
| Belt Size (*n*) | HOMO-2 | HOMO-1 | HOMO | LUMO | LUMO+1 | LUMO+2 | HOMO-2 | HOMO-1 | HOMO | LUMO | LUMO+1 | LUMO+2 |
| 5 | 2.00 | 1.76 | 1.75 | 0.47 | 0.01 | 0.01 | 2.00 | 2.00 | 1.81 | 0.19 | 0.00 | 0.00 |
| 6 | 2.00 | 2.00 | 1.68 | 0.27 | 0.05 | 0.00 | 2.00 | 2.00 | 1.93 | 0.06 | 0.02 | 0.00 |
| 7 | 2.00 | 1.73 | 1.73 | 0.27 | 0.27 | 0.00 | 2.00 | 2.00 | 1.90 | 0.09 | 0.01 | 0.00 |
| 8 | 1.99 | 1.99 | 1.69 | 0.31 | 0.01 | 0.01 | 2.00 | 2.00 | 1.79 | 0.21 | 0.00 | 0.00 |
| 9 | 2.00 | 1.36 | 1.36 | 0.69 | 0.68 | 0.00 | 2.00 | 2.00 | 1.68 | 0.31 | 0.01 | 0.00 |
| 10 | 1.96 | 1.96 | 1.69 | 0.32 | 0.03 | 0.03 | 2.00 | 1.99 | 1.47 | 0.54 | 0.01 | 0.00 |
| 11 | 2.00 | 1.01 | 1.01 | 1.00 | 0.99 | 0.00 | 2.00 | 1.98 | 1.35 | 0.63 | 0.04 | 0.00 |
| 12 | 1.88 | 1.88 | 1.70 | 0.33 | 0.10 | 0.10 | 2.00 | 1.94 | 1.16 | 0.87 | 0.04 | 0.00 |
| 13 | 1.99 | 1.21 | 1.21 | 0.80 | 0.79 | 0.01 | 2.00 | 1.93 | 1.06 | 0.90 | 0.12 | 0.00 |
| 14 | 1.72 | 1.72 | 1.70 | 0.34 | 0.26 | 0.26 | 1.99 | 1.82 | 1.25 | 0.81 | 0.12 | 0.01 |

Table 8. Frontier active orbital occupation numbers for the TAO-DFT electronic structures of the Möbius-[n]cyclacene isomers with only Kekulé benzenoid rings (KB) and one Dewar benzenoid ring (DB). The occupations have been doubled in order to account for both spin densities.

| | Möbius KB | | | | | | Möbius DB | | | | | |
|---|---|---|---|---|---|---|---|---|---|---|---|---|
| Belt Size (*n*) | HOMO-2 | HOMO-1 | HOMO | LUMO | LUMO+1 | LUMO+2 | HOMO-2 | HOMO-1 | HOMO | LUMO | LUMO+1 | LUMO+2 |
| 9 | 2.00 | 1.77 | 1.50 | 0.71 | 0.03 | 0.00 | 2.00 | 1.97 | 1.09 | 0.93 | 0.01 | 0.00 |
| 10 | 1.97 | 1.95 | 1.31 | 0.54 | 0.23 | 0.00 | 2.00 | 1.96 | 1.31 | 0.65 | 0.09 | 0.00 |
| 11 | 2.00 | 1.76 | 1.32 | 0.80 | 0.10 | 0.02 | 1.97 | 1.61 | 0.31 | 0.11 | 0.01 | 0.00 |
| 12 | 1.87 | 1.81 | 1.30 | 0.75 | 0.28 | 0.00 | 1.99 | 1.86 | 1.04 | 0.92 | 0.19 | 0.00 |
| 13 | 1.99 | 1.78 | 1.00 | 0.86 | 0.29 | 0.10 | 1.98 | 1.83 | 1.34 | 0.72 | 0.12 | 0.01 |
| 14 | 1.68 | 1.61 | 1.37 | 1.03 | 0.29 | 0.01 | 1.98 | 1.68 | 1.23 | 0.75 | 0.34 | 0.01 |

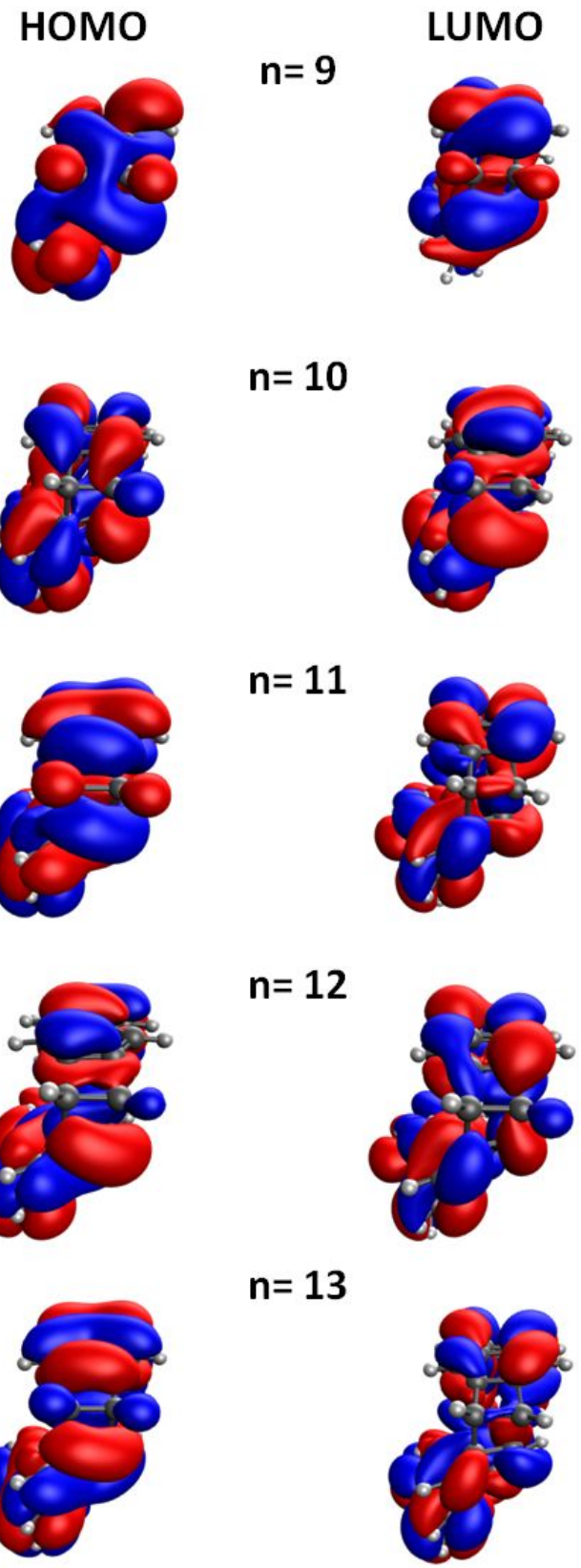


Figure 4. Frontier canonical DFT orbitals for several Möbius-[n]cyclacene isomers containing a Dewar benzenoid ring. The HOMO is defined here as the $(N/2)^{th}$ orbital and LUMO is defined as the $(N/2+1)^{th}$ orbital, the orbitals are shown at an isosurface value of 0.02 e/Å$^3$, and the molecule has been angled with the centre of the DB facing out-of-plane.

## Conclusions

The Hückel-[5]cyclacene isomer containing two maximally spaced Ladenburg benzenoid rings is predicted to be more stable than the conventional purely Kekulé benzenoid ring isomer. Hückel-[n]cyclacene isomers containing Ladenburg benzenoid rings are then less stable in general compared to the isomers of equal size that contain either Dewar benzenoid rings or purely Kekulé benzenoid rings, and Hückel-[n]cyclacene isomers containing any of the defects studied are less stable than their purely Kekulé benzenoid ring isomer counterparts for the $n$ = 8-14 belt sizes. The introduction of a single Dewar benzenoid defect into a Möbius-[n]cyclacene nanobelt is predicted to lower the energy of the system to a greater degree than their introduction into the equivalent Hückel-[n]cyclacene. The Möbius-[9]cyclacene isomer containing a single Dewar benzenoid ring is predicted to be the most stable Möbius structure, and the presence of both Dewar and Ladenburg benzenoid defects increases the energy difference between the lowest singlet and triplet electronic states while also decreasing the calculated radical character for the isomers studied. The high relative energies of these isomers limit their experimental viability. However, understanding the properties that these defects introduce is an important consideration for modelling cyclacene dynamics under idealized conditions, and when determining the viability of the potential synthetic pathways that contain them.

## ASSOCIATED CONTENT

### Supporting Information

The Supporting Information is available free of charge at https://pubs.acs.org/doi/...

Calculated absolute energies and Cartesian coordinates for the optimized geometries of the new [n]cyclacene isomers studied.

### Author Information

**Corresponding Author**

*E-mail: magnus.hansonheine@nottingham.ac.uk.

**ORCID**

Magnus W. D. Hanson-Heine: 0000-0002-6709-297X

Jonathan D. Hirst: 0000-0002-2726-0983

**Notes**

The author declares no competing financial interest.

**Acknowledgements**

We thank the University of Nottingham Green Chemicals Beacon for funding toward this research.

**References**

1. Heilbronner, E., Molecular Orbitals in homologen Reihen mehrkerniger aromatischer Kohlenwasserstoffe: I. Die Eigenwerte von LCAO-MO's in homologen Reihen. *Helv. Chim. Acta* **1954,** *37* (3), 921-935.

2. Tahara, K.; Tobe, Y., Molecular Loops and Belts. *Chem. Rev.* **2006,** *106* (12), 5274-5290.

3. Türker, L.; Gümüş, S., Cyclacenes. *J. Mol. Struct. (Theochem)* **2004,** *685* (1), 1-33.

4. Türker, L., Cryptoannulenic Behavior of Cyclacenes. *Polycyclic Aromat. Compd.* **1994,** *4* (3), 191-197.

5. Povie, G.; Segawa, Y.; Nishihara, T.; Miyauchi, Y.; Itami, K., Synthesis of a carbon nanobelt. *Science* **2017,** *356* (6334), 172-175.

6. Kohnke, F. H.; Slawin, A. M. Z.; Stoddart, J. F.; Williams, D. J., Molecular Belts and Collars in the Making: A Hexaepoxyoctacosahydro[12]cyclacene Derivative. *Angew. Chem. Int. Ed.* **1987,** *26* (9), 892-894.

7. Ashton, P. R.; Isaacs, N. S.; Kohnke, F. H.; Slawin, A. M. Z.; Spencer, C. M.; Stoddart, J. F.; Williams, D. J., Towards the Making of [12]Collarene. *Angew. Chem. Int. Ed.* **1988,** *27* (7), 966-969.

8. Ashton, P. R.; Brown, G. R.; Isaacs, N. S.; Giuffrida, D.; Kohnke, F. H.; Mathias, J. P.; Slawin, A. M. Z.; Smith, D. R.; Stoddart, J. F.; Williams, D. J.,

Molecular LEGO. 1. Substrate-directed synthesis via stereoregular Diels-Alder oligomerizations. *J. Am. Chem. Soc.* **1992,** *114* (16), 6330-6353.

9. Cory, R. M.; McPhail, C. L.; Dikmans, A. J.; Vittal, J. J., Macrocyclic cyclophane belts via double Diels-Alder cycloadditions: Macroannulation of bisdienes by bisdienophiles. Synthesis of a key precursor to an 8 cyclacene. *Tetrahedron Lett.* **1996,** *37* (12), 1983-1986.

10. Schulz, F.; García, F.; Kaiser, K.; Pérez, D.; Guitián, E.; Gross, L.; Peña, D., Exploring a Route to Cyclic Acenes by On-Surface Synthesis. *Angew. Chem. Int. Ed.* **2019,** *58* (27), 9038-9042.

11. Matsui, K.; Fushimi, M.; Segawa, Y.; Itami, K., Synthesis, Structure, and Reactivity of a Cylinder-Shaped Cyclo 12 orthophenylene 6 ethynylene: Toward the Synthesis of Zigzag Carbon Nanobelts. *Org. Lett.* **2016,** *18* (20), 5352-5355.

12. Sadowsky, D.; McNeill, K.; Cramer, C. J., Electronic structures of [n]-cyclacenes (n = 6–12) and short, hydrogen-capped, carbon nanotubes. *Faraday Discuss.* **2010,** *145* (0), 507-521.

13. Battaglia, S.; Faginas-Lago, N.; Andrae, D.; Evangelisti, S.; Leininger, T., Increasing Radical Character of Large [n]cyclacenes Unveiled by Wave Function Theory. *J. Phys. Chem. A* **2017,** *121* (19), 3746-3756.

14. Irle, S.; Mews, A.; Morokuma, K., Theoretical Study of Structure and Raman Spectra for Models of Carbon Nanotubes in Their Pristine and Oxidized Forms. *J. Phys. Chem. A* **2002,** *106* (49), 11973-11980.

15. Quiñonero, D.; Frontera, A.; Garau, C.; Costa, A.; Ballester, P.; Deyà, P. M., Ab initio investigations of lithium insertion in boron and nitrogen-doped single-walled carbon nanotubes. *Chem. Phys. Lett.* **2005,** *411* (1), 256-261.

16. Jasti, R.; Bertozzi, C. R., Progress and challenges for the bottom-up synthesis of carbon nanotubes with discrete chirality. *Chem. Phys. Lett.* **2010,** *494* (1), 1-7.

17. Heilbronner, E., Hűckel molecular orbitals of Mőbius-type conformations of annulenes. *Tetrahedron Lett.* **1964,** *5* (29), 1923-1928.

18. Ajami, D.; Oeckler, O.; Simon, A.; Herges, R., Synthesis of a Möbius aromatic hydrocarbon. *Nature* **2003,** *426* (6968), 819-821.

19. Rzepa, H. S., Möbius Aromaticity and Delocalization. *Chem. Rev.* **2005,** *105* (10), 3697-3715.

20. Stępień, M.; Latos-Grażyński, L.; Sprutta, N.; Chwalisz, P.; Szterenberg, L., Expanded Porphyrin with a Split Personality: A Hückel–Möbius Aromaticity Switch. *Angew. Chem. Int. Ed.* **2007,** *46* (41), 7869-7873.

21. Tanda, S.; Tsuneta, T.; Okajima, Y.; Inagaki, K.; Yamaya, K.; Hatakenaka, N., A Möbius strip of single crystals. *Nature* **2002,** *417* (6887), 397-398.

22. Dias, J. R., Comprehensive study of the correlations that exist among the members of the [n]cyclacene series and the Möbius[n]cyclacene series. *Mol. Phys.* **2018,** *116* (4), 423-448.

23. Xing, S.-K.; Li, Y.; Zhao, X.-Z.; Cai, Z.-S.; Shang, Z.-F.; Wang, G.-C., Molecular Symmetry of Mobius Cyclacenes. *Acta Phys. -Chim. Sin.* **2011,** *27* (05), 1000-1004.

24. dos Santos, M. C.; Alvarez, F., Spin current in the Möbius cyclacene belts. *Chem. Phys. Lett.* **2009,** *471* (4), 276-279.

25. Gao, Y.; Xu, H.-L.; Zhong, R.-L.; Sun, S.-L.; Su, Z.-M., Structures and electro-optical properties of Möbius [n]Cyclacenes[13–18]: a theoretical study. *J. Mol. Model.* **2014,** *20* (4), 2201.

26. Zhong, R.-L.; Xu, H.-L.; Su, Z.-M.; Li, Z.-R.; Sun, S.-L.; Qiu, Y.-Q., Spiral Intramolecular Charge Transfer and Large First Hyperpolarizability in Möbius Cyclacenes: New Insight into the Localized π Electrons. *ChemPhysChem* **2012,** *13* (9), 2349-2353.

27. Chen, L.; Yu, G.; Chen, W.; Tu, C.; Zhao, X.; Huang, X., Constructing a mixed π-conjugated bridge to effectively enhance the nonlinear optical response in the Möbius cyclacene-based systems. *Phys. Chem. Chem. Phys.* **2014,** *16* (22), 10933-10942.

28. Jiang, D.-e.; Dai, S., Spin States of Zigzag-Edged Möbius Graphene Nanoribbons from First Principles. *J. Phys. Chem. C* **2008,** *112* (14), 5348-5351.

29. Chung, J.-H.; Chai, J.-D., Electronic Properties of Möbius Cyclacenes Studied by Thermally-Assisted-Occupation Density Functional Theory. *Sci. Rep.* **2019,** *9* (1), 2907.

30. Van Tamelen, E. E.; Pappas, S. P., Chemistry of Dewar Benzene. 1,2,5-Tri-t-Butylbicyclo[2.2.0]Hexa-2,5-Diene. *J. Am. Chem. Soc.* **1962,** *84* (19), 3789-3791.

31. Katz, T. J.; Acton, N., Synthesis of prismane. *J. Am. Chem. Soc.* **1973,** *95* (8), 2738-2739.

32. Katz, T. J.; Roth, R. J.; Acton, N.; Carnahan, E. J., Synthesis of Benzvalene. *J. Org. Chem.* **1999,** *64* (20), 7663-7664.

33. Katz, T. J.; Wang, E. J.; Acton, N., Benzvalene synthesis. *J. Am. Chem. Soc.* **1971,** *93* (15), 3782-3783.

34. Hanson-Heine, M. W. D.; Rogers, D. M.; Woodward, S.; Hirst, J. D., Dewar Benzenoids Discovered In Carbon Nanobelts. *J. Phys. Chem. Lett.* **2020,** 11, 3769-3772.

35. Shao, Y.; Gan, Z.; Epifanovsky, E.; Gilbert, A. T. B.; Wormit, M.; Kussmann, J.; Lange, A. W.; Behn, A.; Deng, J.; Feng, X., et al., Advances in molecular quantum chemistry contained in the Q-Chem 4 program package. *Mol. Phys.* **2014,** *113* (2), 184-215.

36. Becke, A. D., Density-functional thermochemistry. III. The role of exact exchange. *J. Chem. Phys.* **1993,** *98* (7), 5648-5652.

37. Stephens, P. J.; Devlin, F. J.; Chabalowski, C. F.; Frisch, M. J., Ab-Initio calculation of vibrational absorption and circular-dichroism spectra using density-functional force-fields. *J. Phys. Chem.* **1994,** *98* (45), 11623-11627.

38. Chai, J.-D., Density functional theory with fractional orbital occupations. *J. Chem. Phys.* **2012,** *136* (15), 154104.

39. Wu, C.-S.; Chai, J.-D., Electronic Properties of Zigzag Graphene Nanoribbons Studied by TAO-DFT. *J. Chem. Theory Comput.* **2015,** *11* (5), 2003-2011.

40. Chai, J.-D., Thermally-assisted-occupation density functional theory with generalized-gradient approximations. *J. Chem. Phys.* **2014,** *140* (18), 18A521.

41. Wu, C.-S.; Lee, P.-Y.; Chai, J.-D., Electronic Properties of Cyclacenes from TAO-DFT. *Sci. Rep.* **2016,** *6*, 37249.

42. Hanson-Heine, M. W. D., Static correlation in vibrational frequencies studied using thermally-assisted-occupation density functional theory. *Chem. Phys. Lett.* **2020,** *739*, 137012.

43. Fosso-Tande, J.; Nguyen, T.-S.; Gidofalvi, G.; DePrince, A. E., Large-Scale Variational Two-Electron Reduced-Density-Matrix-Driven Complete Active Space Self-Consistent Field Methods. *J. Chem. Theory Comput.* **2016,** *12* (5), 2260-2271.

44. Yeh, C.-N.; Chai, J.-D., Role of Kekulé and Non-Kekulé Structures in the Radical Character of Alternant Polycyclic Aromatic Hydrocarbons: A TAO-DFT Study. *Sci. Rep.* **2016,** *6*, 30562.

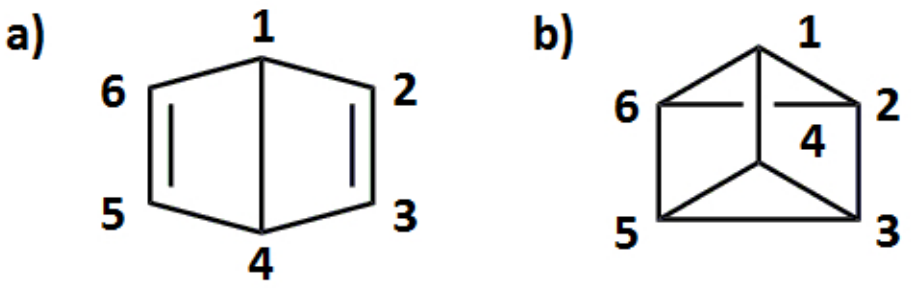


Figure 1. Chemical structures of a) Dewar benzene and b) Ladenburg benzene (prismane).

137x41mm (96 x 96 DPI)

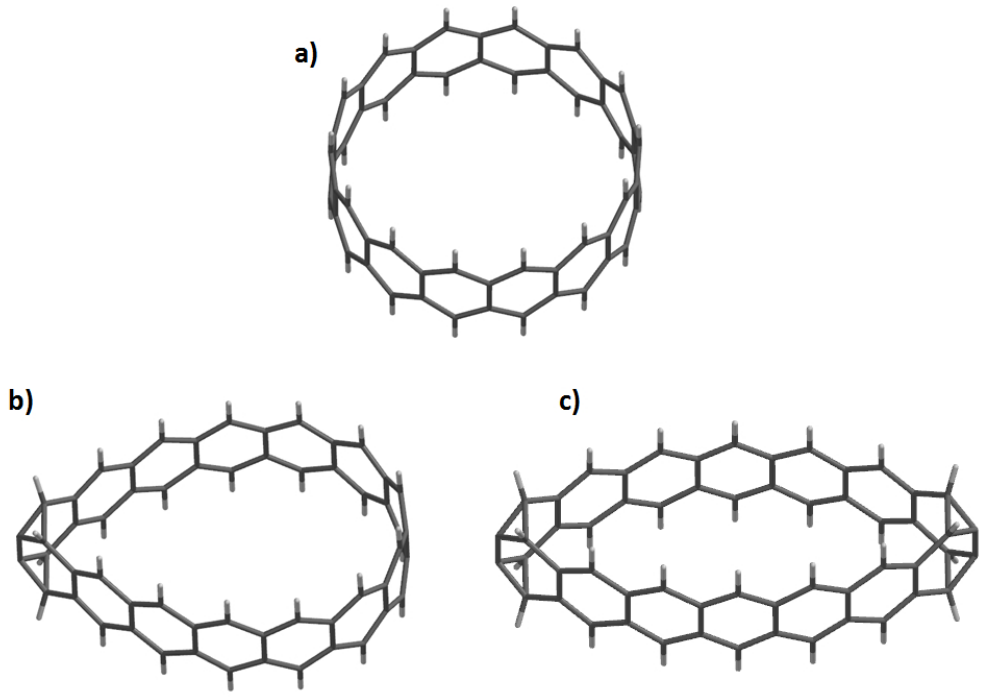


Figure 2. Optimized geometries of the 14-cyclacene isomers studied containing a) only Kekulé benzenoids, b) one Ladenburg benzenoid, and c) two Ladenburg benzenoids.

254x177mm (96 x 96 DPI)

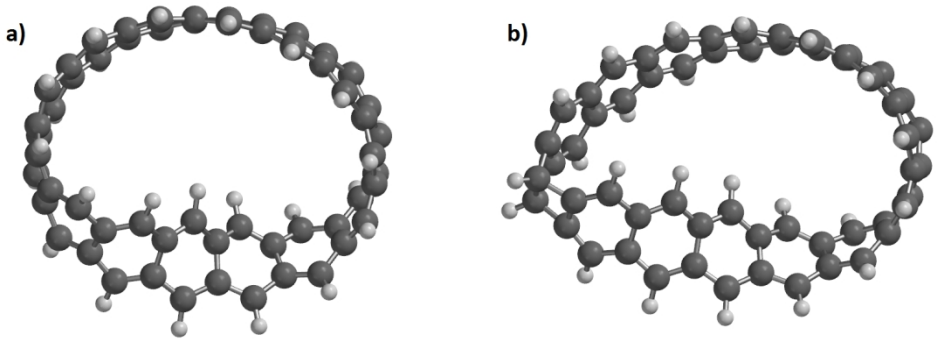


Figure 3. Optimized geometries of the Möbius-[14]cyclacene isomers studied containing a) Kekulé benzenoids only and b) a single Dewar benzenoid.

446x155mm (96 x 96 DPI)

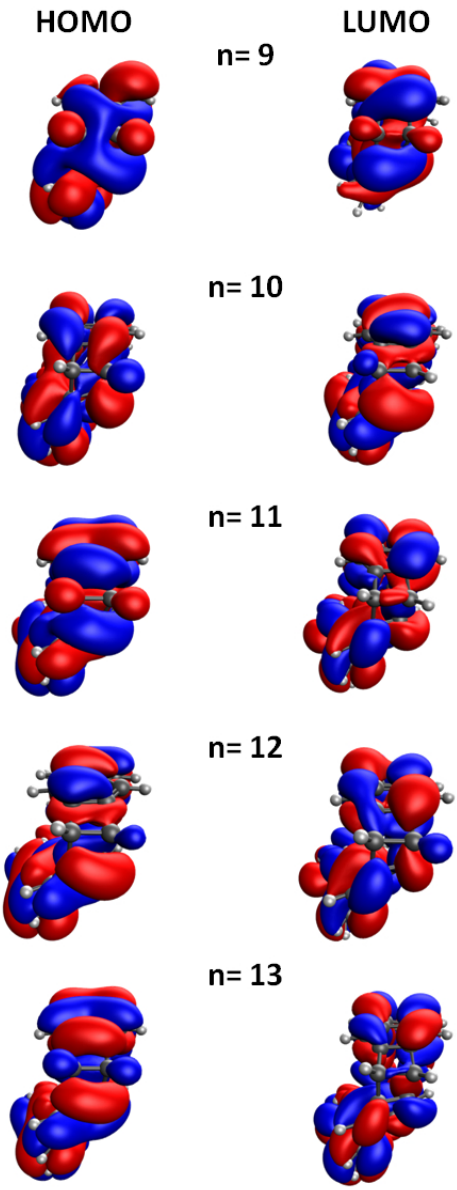


Figure 4. Frontier canonical DFT orbitals for several Möbius-[n]cyclacene isomers containing a Dewar benzenoid. The HOMO is defined here as the (N/2)th orbital and LUMO is defined as the (N/2+1)th orbital, the orbitals are shown at an isosurface value of 0.02 e/Å3, and the molecule has been angled with the centre of the DB facing out-of-plane.

121x297mm (96 x 96 DPI)

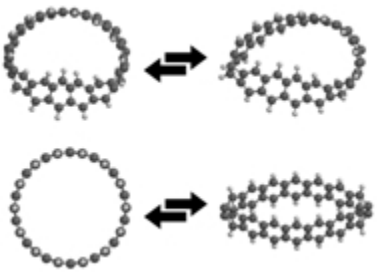

TOC Graphic

50x35mm (96 x 96 DPI)